Weather and Climate Extremes 42 (2023) 100604

Contents lists available at ScienceDirect

Weather and Climate Extremes

journal homepage: www.elsevier.com/locate/wace

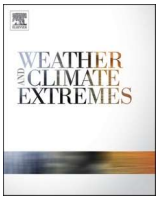

Changes in design precipitation over the Nordic-Baltic region as given by convection-permitting climate simulations

Anita Verpe Dyrrdal [a,*], Erika Médus [b], Andreas Dobler [a], Øivind Hodnebrog [c], Karsten Arnbjerg-Nielsen [d], Jonas Olsson [e], Emma Dybro Thomassen [f], Petter Lind [g], Dace Gaile [h], Piia Post [i]

[a] Norwegian Meteorological Institute, Norway
[b] Finnish Meteorological Institute, Finland
[c] CICERO Center for International Climate Research, Norway
[d] Technical University of Denmark, Denmark
[e] Swedish Meteorological and Hydrological Institute and Lund University, Sweden
[f] Technical University of Denmark and Danish Meteorological Institute, Denmark
[g] Swedish Meteorological and Hydrological Institute, Sweden
[h] Latvian Environment, Geology and Meteorology Centre, Latvia
[i] University of Tartu, Estonia

A B S T R A C T

The increased risk of flooding due to global warming and subsequent heavy rainfall events in the Nordic-Baltic region, call for recommendations directed at long-term planning. One example of such recommendations are climate change allowances. These are often based on expected changes in design precipitation as given by climate model simulations, and are used as a buffer on top of current design values to avoid a future increased damage potential as a consequence of climate change. We here compute expected changes in precipitation design values, so-called climate factors (CFs), for the Nordic-Baltic region, based on 3 km convection permitting simulations from the Nordic Convection Permitting Climate Projections project. These have the advantage of explicitly resolving convection, which has been shown to be the main contributor to increased rainfall. We assess the dependence of the CFs on rainfall duration, return period, and geographical location, focusing on the summer (convective) season, short durations and the high emission scenario RCP8.5. We also compare these CFs to those computed from a non-convection permitting regional climate model ensemble.

We found higher CFs for the longer return period, with only few exceptions, and distinctly higher CFs going from daily to sub-daily durations. However, the different simulations give conflicting results for very short-duration rainfall (<3 h). The huge difference in the climate sensitivity of driving GCMs dominates the magnitude of estimated return levels. Our analysis is shaped by the high computational costs of running convection permitting models, resulting in a very limited ensemble (3 members) representing a single emission scenario (RCP8.5). Therefore, we believe that combining results from convection permitting simulations with a larger ensemble (21 members) of non-convection permitting simulations adds value to the assessment of robust climate change allowances for heavy precipitation in the Nordic-Baltic region.

1. Introduction

Climatic changes lead to increased heavy precipitation and subsequent pluvial flooding and landslides due to overloading of e.g. urban water infrastructure (Willems et al., 2012). Societies in general, and urban planners and water engineers in particular, need to be informed about the size of these changes in order to develop policies and best practices to manage the enhanced risk associated with more intense and more frequent rainfall (Madsen et al., 2018). Precipitation design values are most often estimated as a function of a return period, indicating the average recurrence interval in years of a certain event. To describe how expected future changes in precipitation may affect design values, so-called "climate factors" for heavy rainfall may be computed (Arnbjerg-Nielsen, 2012). A climate factor (CF) is defined as the relative change in design values, in our case for precipitation, between a past and a future climate period. Some Nordic countries have implemented recommendations for the design of infrastructure and long-term planning based on climate factors, often referred to as climate change allowance. In Finland a general climate change allowance of 1,20 is suggested (Kuntaliitto, 2012), in Sweden 1,20–1,25 is recommended depending on

* Corresponding author.
E-mail address: anitavd@met.no (A.V. Dyrrdal).

https://doi.org/10.1016/j.wace.2023.100604
Received 8 March 2023; Received in revised form 17 August 2023; Accepted 17 August 2023
Available online 26 August 2023

the duration of the intensity considered (Svenskt Vatten, 2016), in Norway 1,30–1,50 is recommended depending on duration and return period (Sorteberg et al., 2018; klimaservicesenter. no), and in Denmark 1,20–1,40 is recommended depending on the return period (Spildevandskomiteen, 2014). All of these recommendations are based on Regional Climate Models (RCMs) with a spatial resolution of 10–25 km or Global Climate Models (GCMs) of coarser resolution, except for a few RCM simulations in Denmark using a spatial resolution of 6 km. To this date, the Baltic countries do not recommend the use of climate change allowances. In this paper we study expected future changes in heavy precipitation over the entire Nordic-Baltic region, as given by a novel set of high resolution climate model simulations.

In the Nordic-Baltic region, an increase in annual maxima of both daily (Dyrrdal et al., 2021) and sub-daily (Olsson et al., 2022; Tamm et al., 2023) precipitation has been observed during the last decades and for the daily duration also changes in seasonal occurrences were observed. Global and regional climate models indicate that these changes in seasonality will continue into the future (Marelle et al., 2018; Christensen et al., 2022). Myhre et al. (2019) indicate that the increase in total precipitation is mainly explained by an increase in the frequency of heavy precipitation events, and that the increase of mean intensity is less significant. Others have found a pronounced intensification in heavy precipitation events (e.g. Fischer and Knutti, 2014; Benestad et al., 2019). In Benestad et al. (2022), the spatial extent of individual precipitation systems over the globe was shown to have decreased while becoming more intense throughout the period 1950–2020, suggesting an acceleration of the rate of the global hydrological cycle. This, in turn, indicates a transition to more intense small-scale precipitation events. Conflicting conclusions are brought forward by Matte et al. (2022) when studying future precipitation events from regional climate simulations. They found that larger systems become more frequent and larger, while smaller systems become less frequent.

According to the most recent assessment report (AR6) from the Intergovernmental Panel on Climate Change (IPCC) human-induced climate change is likely the main driver of recent past increases in heavy precipitation, and they state that under additional global warming more intense and frequent heavy precipitation events are very likely in most regions (IPCC et al., 2021). Northern Europe is, according to this report, among the regions with the most confident precipitation increase. Fisher and Knutti (2016) point out that the response of precipitation to increased greenhouse gas concentrations and consequent warming is complex, and different rainfall intensities often respond differently to warming. Sillmann et al. (2019) also showed that the extremes respond differently depending on the climate driver (e.g. greenhouse gasses vs. aerosols).

Many studies have shown that short-duration, high-intensity events, often resulting from convection, increase more as the atmosphere warms, compared to lower intensity events (Fowler et al., 2021; Hodnebrog et al., 2019; Myhre et al., 2019). Such convective events are often local and fast evolving, and traditional Regional Climate Models at scales of 10 km or more cannot resolve this behavior explicitly (Westra et al., 2014). Instead so-called convection permitting (CP) models with a spatial scale of a few kilometers are suggested (e.g. Prein et al., 2015; Kendon et al., 2017; Ban et al., 2021). CP models applied at 1–4 km grid spacing have in many cases proven to give added value compared to coarser-scale models (Lind et al., 2020; Lucas-Picher et al., 2021; Olsson et al., 2021). The Nordic Convection Permitting Climate Projections project (NorCP; Lind et al., 2020) uses the HARMONIE-Climate regional climate model, cycle 38 (HCLIM38), to run at a convection-permitting scale of 3 km grid spacing over Northern Europe, with an intermediate nesting step at 12 km grid spacing (Belušić et al., 2020). According to Lind et al. (2020), the 3 km simulations strongly improve the representation of precipitation compared to the 12 km simulations, mostly through reduced "drizzle" and more frequent high intensity events. In a reanalysis study Médus et al. (2022) found that HCLIM38 well represents daily heavy precipitation amounts and frequencies, as well as daily return levels over the Nordic region. Further, the 3 km simulation is able to capture the most intense hourly precipitation events and their frequency with a slight overestimation, while these are underestimated at 12 km.

Within the NorCP project, two GCMs were dynamically downscaled with HCLIM38 to 12 km and 3 km. The two GCMs; EC-EARTH (Hazeleger et al., 2011) and GFDL-CM3 (hereby GFDL; Griffies et al., 2011; Donner et al., 2011) were selected to cover a spread from medium to large climate change response in terms of temperature, respectively (Lind et al., 2022). Due to the high computational costs of running a climate model at a spatial resolution of 3 km covering the whole of Fennoscandia, the downscaling is limited to three 20-year time slices; 1986–2005, 2041–2060 and 2081–2100, and to the high emission scenario RCP8.5 (both GCMs) and the medium emission scenario RCP4.5 (only one GCM). Lind et al. (2022) studied climate change over Fennoscandia as projected by these NorCP simulations. They found that the warmer and wetter climate conditions simulated in the GCMs lead to increased precipitation in fall, winter and spring, while in summer, small changes or even decreases are seen in the southern parts of Fennoscandia. Both daily and sub-daily intense precipitation becomes more frequent at the expense of low-intensity events, and HCLIM38 at the CP scale (3 km) gives a significantly stronger increase in summer hourly precipitation extremes compared to the 12 km simulations.

The new simulations used in this paper are compared to an EURO-CORDEX RCM ensemble of 21 members (~12 km). To assess the degree of model dependency on the differences between HCLIM38 and EURO-CORDEX, we also compare CFs for Southern Norway to CFs from independent simulations by the Weather Research and Forecasting (WRF) model (Skamarock and Klemp, 2008) at 3 km resolution. In addition to the effect of model resolution (CP or not), we address the spatial distribution of CFs and how CFs change with duration and return period. According to Lind et al. (2022), there is a smaller GCM control of summer precipitation compared to other variables, and as urban flooding often results from heavy rainfall over short durations, we here focus on heavy summer precipitation on minute-to-hour scales.

2. Data and method

2.1. Climate simulations

In the current paper we focus on changes between the reference period 1986–2005 and the end of the century; 2081–2 100 under the high emission scenario RCP8.5. This is also adequate for the long planning horizon of infrastructure design (e.g. DMI, 2018). The available temporal output resolution for precipitation from the HCLIM38 simulations is 15 min for 3 km and 1 h for 12 km. Based on the different model configurations used (see Belušić et al., 2020) we refer to the convection-permitting 3 km HCLIM38 simulations as AROME and the 12 km HCLIM38 simulations as ALADIN in the following. The ALADIN and AROME simulations downscaled from EC-EARTH are referred to AladinE and AromeE, while those downscaled from GFDL are referred to as AladinG and AromeG. Details on the model simulations addressed in the current paper are presented in Table 1. Between 1986-2005 and 2081–2100, EC-EARTH projects a warming of 3.57° over North Europe for the calendar summer (June-July-August; hereby JJA). GFDL represents the high end of projected climate change, with a warming of 6.76°, more than two degrees higher than the global mean.

From Table 1 we also find that EC-EARTH projects a 9.71% increase in average total summer precipitation in North Europe. GFDL projects a change of only 3.74% during summer over North Europe, while for the whole year a very large change of 23.79% is projected. This strong increase was also noted in Lind et al. (2022) showing increases of around 40% in the RCP8.5 scenario for autumn and winter, mainly over Fenno-Scandinavia, the North Sea and the British Isles. These changes are consistent with intensified zonal flow and synoptic activity in the regions in the AladinG simulation (Lind et al., 2022). In summer, Lind

Table 1
Description of climate simulations. CP = convection permitting. Temperature change (ΔT) and precipitation change (ΔP) from the driving GCM represents mean annual and summer changes between 1986-2005 and 2081–2100, globally (upper) and over North Europe (lower) under the emission scenario RCP8.5. North Europe is defined in IPCC AR5 (van Oldenborgh et al., 2013). Grid & output refers to the grid spacing and temporal output resolution. For HCLIM38 and WRF we also report the computing time step of the model (dt).

Acr.	RCM	GCM	Grid & resolution	ΔT from GCM (°)	ΔP from GCM (%)	Reference
EC	EURO-CORDEX ensemble of 21 members (see list in Appendix)	See Appendix	12 km 1 h	–	–	Jacob et al. (2014)
AladinE	HCLIM38-ALADIN	EC-EARTH	12 km 1 h dt = 300 s	3.57/3.38 3.98/3.57	6.58/6.75 11.63/9.71	Lind et al. (2022)
AladinG	HCLIM38-ALADIN	GFDL-CM3	12 km 1 h dt = 300 s	4.72/4.67 6.13/6.76	8.41/8.97 23.79/3.74	Lind et al. (2022)
AromeE	HCLIM38-AROME	EC-EARTH	3 km (CP) 15 min dt = 75 s	3.57/3.38 3.98/3.57	6.58/6.75 11.63/9.71	Lind et al. (2022)
AromeG	HCLIM38-AROME	GFDL-CM3	3 km (CP) 15 min dt = 75 s	4.72/4.67 6.13/6.76	8.41/8.97 23.79/3.74	Lind et al. (2022)
WRF	WRF	CESM1-CAM4	3 km (CP) 10 min dt = 20 s	3.12/3.08 2.21/2.37	5.07/4.68 3.75/−12.7	Hodnebrog et al. (2019)

et al. (2016) show that humidity in AladinG is not increasing along with the strong warming over southern parts of Fenno-Scandinavia, leading to a limited moisture availability and thus a smaller change in summer precipitation.

In a recent review of CP modeling by Lucas-Picher et al. (2021) several concerns were raised, two of them relating to the short periods over which simulations are obtained (time slice mode) and few ensemble members as a result of heavy computational requirements. This is also true for the NorCP simulations. To address the concern of few ensemble members, we include a simulation from the WRF model (Skamarock and Klemp, 2008) in our study, which is run on a convection-permitting 3 km scale nested from 15 km to 45 km resolution domains (Hodnebrog et al., 2019) with boundary conditions provided from CESM1-CAM4 (Gent et al., 2011). Available temporal output resolution for precipitation is 10 min. According to Table 1, CESM1-CAM4 projects summer temperatures to increase by 2.37° over North Europe, somewhat smaller than the global mean. This is most likely due to a strong North Atlantic warming hole in CAM4 (Meehl et al., 2012). A relatively large decrease of 12.7% in summer precipitation is projected over North Europe. WRF simulations do not cover the whole Nordic-Baltic domain, but are here analyzed for Southern Norway (Fig. 2).

Fig. 1 is downloaded from the GCMeval tool online (Parding et al., 2020) and places the three driving GCMs; EC-EARTH, GFDL and CCSM4 (replacing CESM1-CAM4) among other RCP8.5 simulations. CESM1-CAM4 is not available in GCMeval, but we assume CCSM4 to give comparable changes as the two model versions are essentially the same. The green color of our three GCMs imply that they all evaluate well over North Europe, compared to other models. Note that the periods compared in GCMeval (1981–2010 and 2071–2 100) differ from periods used in this study.

2.2. Computing climate factors

A climate factor (CF) can be expressed as follows

$$CF_{T,d,s} = \frac{Pr_{fut,T,d,s}}{Pr_{hist,T,d,s}} \quad (1)$$

Fig. 1. Average a) annual and b) summer temperature and precipitation change in North Europe between 1981-2010 and 2071–2 100 for different GCMs under the RCP8.5 emission scenario. Driving GCMs for simulations used in this study are shown as "selected models" (from GCMeval). Figures are created in GCMeval (gcmeval.met.no) and colors refer to model ranking according to their representation of the climate of the past given default evaluation criteria of the GCMeval tool (green: high rank, pink: low rank). (For interpretation of the references to color in this figure legend, the reader is referred to the Web version of this article.)

Fig. 2. Map of the domain covered by AROME (green) and WRF (black) simulations. (For interpretation of the references to color in this figure legend, the reader is referred to the Web version of this article.)

where Pr refers to the precipitation design value in terms of return levels, the return period, *T*, duration, d, and season, s, and with fut denoting the future period and hist the historical period. A precipitation return level is the precipitation intensity with a specified probability of occurrence. For instance, a 10-year return level has a 10% probability of occurring each year. The climate factor will also in general depend on the emission scenario and climate model.

To estimate return levels, it is common practice to fit an extreme value distribution (e.g. Coles, 2001), namely a Generalized Extreme Value (GEV) or a Generalized Pareto (GP) distribution, depending on the extreme selection method. A GEV distribution, used here, is fit to block maxima; either annual or seasonal maxima. To estimate the three parameters location, scale and shape, that describe the GEV distribution, we apply a modified Maximum-Likelihood-Estimation (MLE), similar to Médus et al. (2022). The modification lies in restraining the challenging shape parameter according to the method in Martins and Stedinger (2000), to prevent unrealistic values when time series are short. As also noted in Médus et al. (2022), the L-moments method was tested and yielded very similar results to the modified MLE estimates.

Climate factors are computed from the following steps for each available simulation.

1. Re-grid to a common EURO-CORDEX grid (0.11°).
2. Compute annual and seasonal maxima series for the selected durations for each grid point for historical and future periods separately.
3. Fit a GEV distribution to annual/seasonal maxima and estimate design values corresponding to selected return periods for each grid point for historical and future periods separately.
4. Calculate the CF based on the future period (2081–2 100) and the historical period (1986–2005) for each duration, return period, and season for each grid point.

Note that values for longer durations are computed from hourly data, with fixed durations (not sliding). Annual maxima from sliding durations would have given slightly higher values (e.g. Olsson et al., 2019), and different durations might be differently impacted by the underestimation due to the non-sliding approach. However, since the future and historical series are both impacted we assume that the influence on estimated CF-values is small.

For the EURO-CORDEX ensemble (hereby; EC-ensemble) and NorCP simulations, we computed CFs over the Nordic-Baltic region (see map in Fig. 2) for the whole year and each season, for durations 15 min (only AROME), 1 h, 3 h and 1 day and for different return periods up to 100 years. The same computation, restricted to the Southern Norway domain (see Fig. 2) and the summer season, was undertaken for the three convection permitting simulations (AromeE, AromeG and WRF).

2.3. Analysis

In the current paper we focus on the annual and summer (June-July-August; JJA) maxima, daily and sub-daily durations and two return periods; 2 and 100 years. Annual maxima are often input to design value estimation, while summer maxima are of special interest as they often result from convective activity causing intense rain showers. Selected maps for the winter season (December-January-February; DJF) are available in the Appendix. The long return period of 100 years implies an extrapolation far beyond the time series length, resulting in large estimation uncertainty. Short time series is a well known challenge in extreme value estimation, but we chose the 100 year return period because this is, in some regions, the required risk level in stormwater management (e.g. Norway; NVE, 2022; Copenhagen; Arnbjerg-Nielsen et al., 2015).

We assess the magnitude and geographical distribution of CFs from the two AROME simulations and compare these to the non-CP ALADIN simulations and the EC-ensemble, from which climate change allowances have been outlined in some countries, in terms of their dependence on return period and duration. In the comparison we present the spatial median and the interquartile range (25th and 75th percentiles) representing the spatial spread. Since the EC-ensemble is a collection of 21 model simulations which are to be compared to single simulations from AROME and ALADIN, we use two approaches to compute the ensemble spread: 1. The interquartile range of the spatial means from the 21 ensemble members, 2. The mean of the 21 percentiles (25th, 50th and 75th). The latter is referred to as field interquartile range.

We address model dependency through highlighting CFs from ensemble members within the EC-ensemble using the same GCM or RCM as used in NorCP, namely three EC-EARTH driven simulations and two simulations from ALADIN (see Table A1). Model dependency is also addressed when comparing CFs from AROME and WRF. In this exercise we scaled the CFs according to the following equation

$$CF_{scaled} = \frac{CF}{\Delta T} \quad (2)$$

where ΔT is the projected global or northern Europe 2 m temperature increase between 1986-2005 and 2081–2 100 from the driving GCM (see Table 1).

3. Results and discussion

3.1. Reference climate

The 2-year and 100-year return levels for precipitation in the reference period 1986–2005, according to AromeE and AromeG, are shown in Fig. 3. A similar map of interpolated 10-year observation-based return values in Olsson et al. (2021) reveals a comparable pattern, but with the higher values over Denmark and southern Norway slightly skewed towards the east. The 100-year levels in Fig. 3 range between 10 and 20 mm in the northern parts to more than 50 mm in the Baltic region, while the 2-year level stays below 20 mm everywhere. Both spatial distribution and values are very similar between AromeE and AromeG, but AromeG gives slightly higher values. Lind et al. (2022) (for example their Fig. 4) shows that GFDL simulates similar summer (JJA) daily

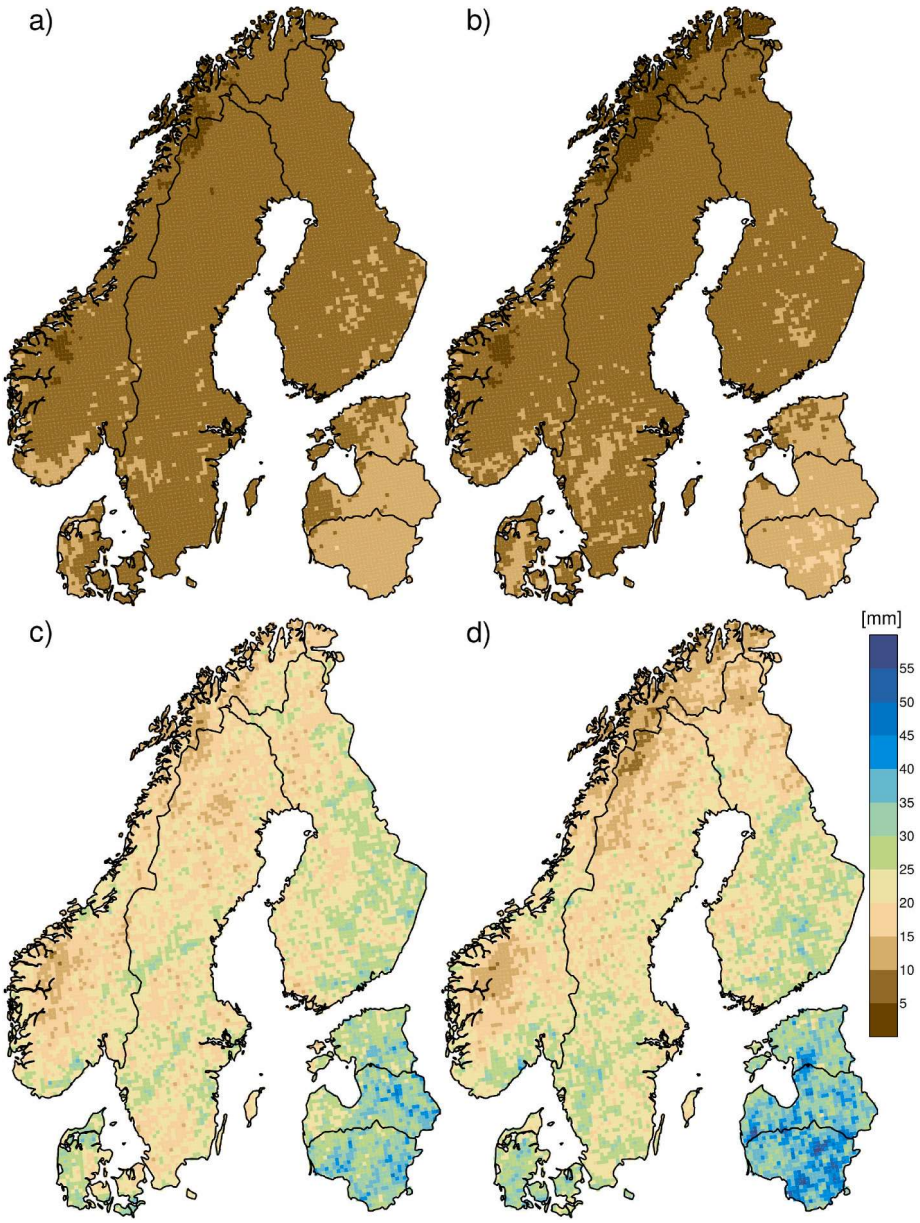

Fig. 3. 2-year (upper) and 100-year (lower) return levels for 1 h summer (JJA) precipitation in the reference period, from AromeE (left) and AromeG (right).

average precipitation amounts as EC-EARTH over Fennoscandia in 1986–2005, while AladinG/AromeG are slightly wetter than AladinE/AromeE. Fig. 3 indicates only minor differences in the 2-year return levels for 1 h precipitation, with slightly larger values in AromeG compared to AromeE over parts of the southern region.

Return levels computed from WRF simulations are presented in Fig. 4, revealing wetter conditions in the reference period compared to AROME. The spatial pattern over Southern Norway is similar between all three simulations.

3.2. Climate factors - comparison between CP and non-CP simulations

In Figs. 5–8 we compare NorCP simulations to the EC-ensemble through boxplots (median and 25–75 percentiles) of CF values for the entire study domain, representing the whole year (Figs. 5 and 6) and summer season only (Figs. 7 and 8). The 2-year return period is shown in Figs. 5 and 7 and the 100-year return period in Figs. 6 and 8. Note that the bars of the EC-ensemble represent the field interquartile range of the 21 ensemble members, as explained under Analysis above, while other bars represent the spatial variability of single simulations.

All simulations give higher median CF-values for longer return periods, although the spread is considerably larger for the 100-year compared to the 2-year return period. The EC-ensemble mean (ECmean) shows increasing CF-values for shorter durations and longer return periods. Higher CFs for longer return periods are in line with the current recommended climate change allowances in Norway and Denmark. Contradicting conclusions were however made for Sweden in Olsson et al. (2017), based on EURO-CORDEX simulations of hourly precipitation, stating no dependency of CFs on the return period. Still, climate factors that are comparable to results in the current paper (RCP8.5, end of the century) are consistently higher for the longer return periods, but given the large uncertainties the authors in Olsson et al. (2017) considered the relatively small differences to be insignificant (personal communication). NorCP simulations also show increasing CFs between 24 h and sub-daily durations, however, values seem to flatten out or even decrease between 1 h and 15 min, except summer 2-year return levels. A larger increase in precipitation for durations around 1 h, if real, might have practical significance as large urban flooding

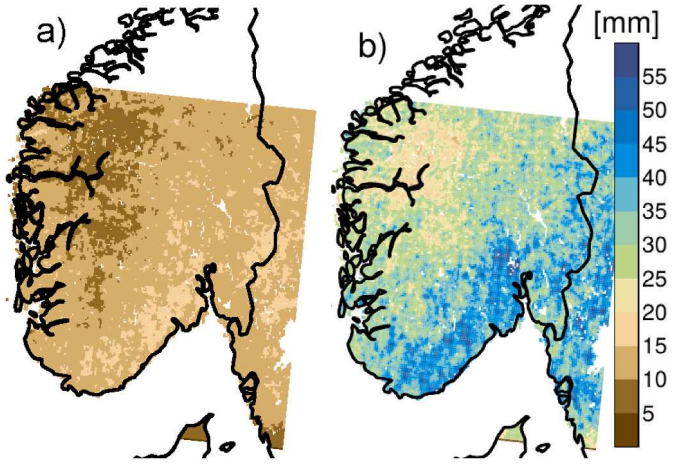

Fig. 4. A) 2-year and b) 100-year return levels for 1 h summer (JJA) precipitation in the reference period from WRF. White spots represent lakes.

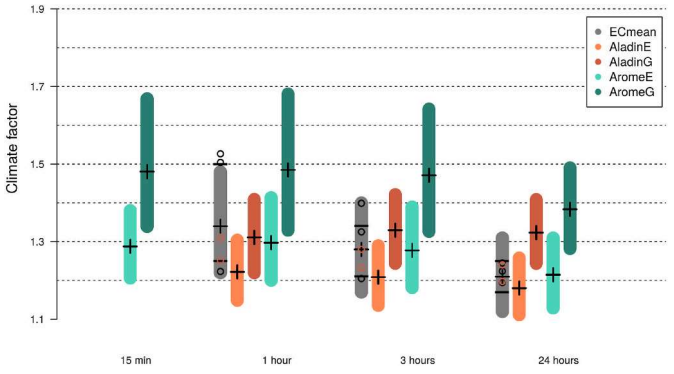

Fig. 5. Annual CFs for the 2-year return level and durations 15 min, 1 h, 3 h and 24 h. Bars represent the spatial interquartile range with the median marked as a plus sign. For the EC-ensemble (grey) bars represent the field interquartile range of the ensemble, while black lines represent the 25th and 75th percentile of the 21 model means.

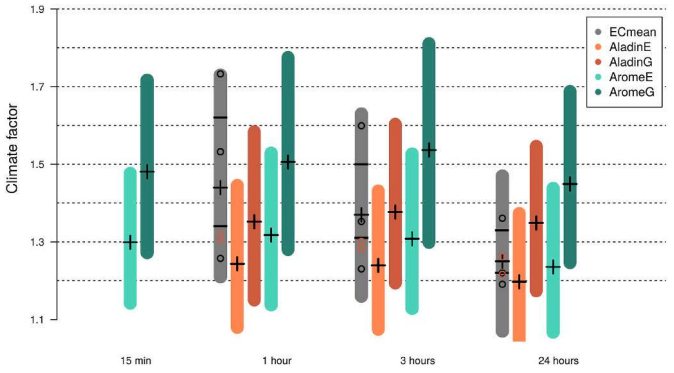

Fig. 6. Similar to Fig. 5, for annual CFs for the 100-year return level and durations 15 min, 1 h, 3 h and 24 h.

events tend to require intense rainfall over a longer time period. The highest CFs are, by far and not surprisingly, seen in the AromeG simulations. In fact, all median CFs are within the spread of the EC-ensemble, as represented by the field interquartile range, except AromeG medians being above the 75th percentile in two thirds of the cases. The interquartile range of the EC model means are, in all cases, much smaller than the field interquartile range.

While AromeG exhibits much higher medians than the ECmean in all

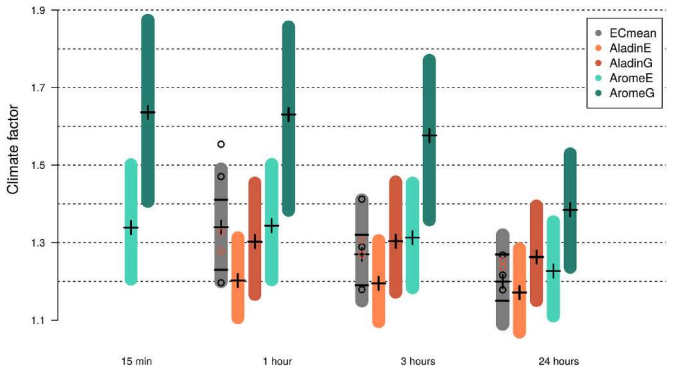

Fig. 7. Similar to Fig. 5 for summer CFs for the 2-year return level and durations 15 min, 1 h, 3 h and 6 h.

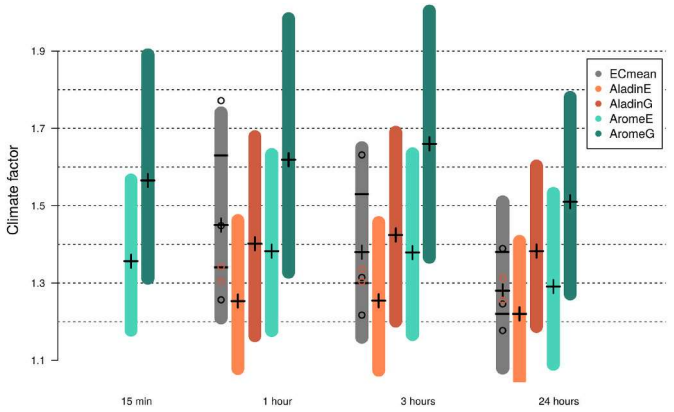

Fig. 8. Similar to Fig. 5 for summer CFs for the 100-year return level and durations 15 min, 1 h, 3 h and 6 h.

cases, medians of AromeE and ECmean are often comparable. The largest exception is for the annual 100-year return level where AromeE gives smaller medians for the 1 and 3 h durations. The variability, represented by the 25th to 75th percentile bars, are similar between the compared simulations, although AromeG has a larger spread overall.

The three EC-EARTH driven simulations from the EC-ensemble are relatively similar for the 24 h duration, however, going to shorter durations they deviate substantially, covering a similar span to the interquartile range of the whole ensemble. This indicates a significant sensitivity to the choice of RCM for precipitation in the Nordic-Baltic region.

The two ALADIN simulations in the EC-ensemble, on the other hand, give relatively similar summer return values over our region. They lie on the higher end of the AromeE range and on the low end of the AromeG range.

Table 2, presenting country-specific spatial average CFs for summer season, the two shortest durations and for all model simulations, reveal a pattern of low CFs from AROME and ALADIN in Denmark, Latvia and Lithuania. The EC-ensemble (ECmean) gives relatively low CFs in Denmark, but values in Latvia and Lithuania are comparable to other countries. Generally, ALADIN simulations give lower values than AROME, in fact, over Fennoscandia values are much lower in AladinG compared to AromeG. Table 2 also provides the EC-ensemble median (ECmed), giving smaller values in all countries compared to ECmean. ECmed have similar CF-values as AromeE (1 h), but are somewhat larger in Denmark and the Baltic countries, except for the 2-year return period in Estonia.

Table 2
Spatial mean CFs for each country for summer (JJA), 10 min (WRF), 15 min (AromeE, AromeG) and 1 h duration. 2/100 year return periods. White (grey) background refers to (non-)convection permitting simulations. Darker blue refers to higher CFs. *Italic: CFs for the 100-year return period < CFs for the 2-year return period.* *Only southern Norway.

	Finland		Sweden		Norway		Denmark		Estonia		Latvia		Lithuania	
WRF* 10m					1.16	1.24								
AromeE 15m	1.32	1.37	1.31	1.37	1.33	1.34	1.10	1.31	1.30	1.45	1.25	1.43	1.25	1.42
AromeG 15m	*1.69*	*1.51*	*1.65*	*1.60*	*1.74*	*1.70*	1.17	1.26	*1.41*	*1.31*	1.17	1.22	1.10	1.18
WRF* 1h					1.12	1.20								
AromeE 1h	1.32	1.39	1.36	1.45	1.36	1.41	1.15	1.34	1.30	1.39	1.23	1.37	1.22	1.33
AromeG 1h	*1.65*	*1.55*	1.66	1.68	1.75	1.77	1.20	1.33	*1.37*	*1.28*	1.11	1.19	1.06	1.12
AladinE 1h	1.23	1.35	1.21	1.34	1.22	1.24	*1.20*	*1.18*	1.17	1.35	1.18	1.35	1.22	1.33
AladinG 1h	1.26	1.35	1.29	1.39	1.40	1.57	1.09	1.09	1.13	1.18	1.13	1.15	*1.15*	*1.14*
ECmed 1h	1.31	1.43	1.32	1.44	1.32	1.42	1.22	1.41	1.29	1.49	1.31	1.44	1.32	1.46
ECmean 1h	1.38	1.55	1.37	1.54	1.34	1.48	1.26	1.45	1.34	1.52	1.39	1.58	1.38	1.57

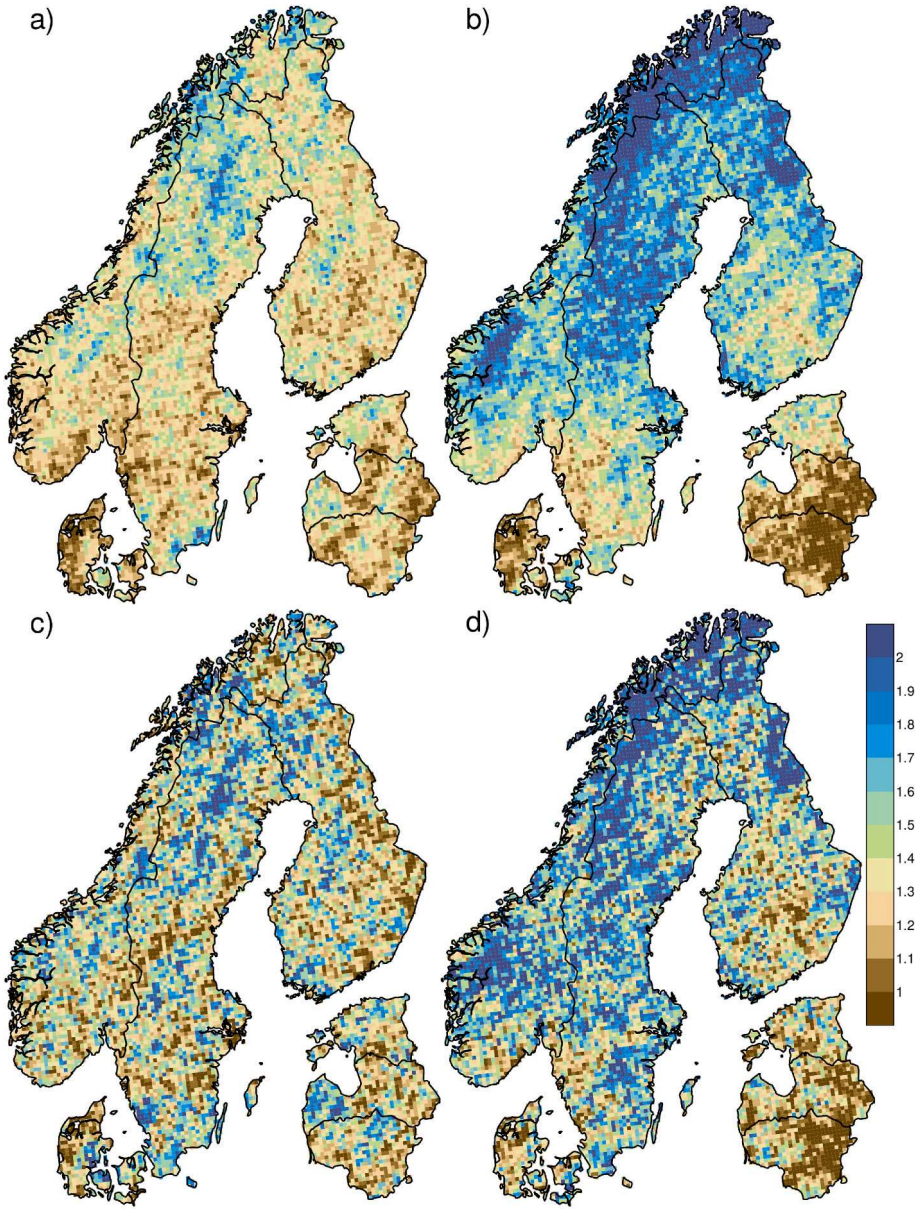

Fig. 9. Climate factors for 2-year (upper) and 100-year (lower) return levels for 1 h summer (JJA) precipitation, from AromeE (left) and AromeG (right).

3.3. Climate factors - comparison between three CP simulations

Fig. 9 presents maps of CFs for the summer (JJA) season and the 2 and 100-year return levels, computed from the two 3 km NorCP simulations with AROME. There is a north to south gradient with higher CFs in the north and lower CFs in the south, and CFs are mostly higher than 1 (indicating increased design precipitation). A slight eastward decrease is also evident when assessing the region as a whole. Given that GFDL has a stronger climate change signal compared to EC-EARTH, AromeG generally exhibits much higher CFs than AromeE. Also, a distinct gradient with very high values are evident in the northeast (northern Norway) while values are very low in the southeast (Latvia and Lithuania). The patchy pattern of the 100-year return level maps (Fig. 3 c and d) implies larger uncertainties, probably associated with the extrapolation to longer return periods. Overall, CFs computed from the 100-year return level are higher than for the 2-year return level in both simulations, implying a stronger increase in summer precipitation extremes. This is in line with former studies as outlined in the Introduction, stating that high-intensity events are expected to increase more compared to the more average low-intensity events. There is however an exception in the northern regions for AromeG, where CFs for the 2-year return period are somewhat higher than for the 100-year return period. In Table 2 we find that this is true for Finland, Sweden and Norway, and partly Estonia. This could be a consequence of the extrapolation to longer return periods given only 20 years of data, and perhaps the larger variability seen in AromeG. To answer the former we investigate the underlying data, i.e. the summer maxima. Considering that the more average summer maxima give basis for the shorter return periods, while the highest summer maxima to a larger degree influence the longer return periods, we compute changes in the median and the highest summer maximum of hourly precipitation at each grid point from AromeG (Table 3). Averaged over Denmark, Latvia and Lithuania, respectively, the largest increases are apparent in the highest summer maxima. The same countries have higher CFs for the 100-year return period compared to the 2-year return period for both 15 min and 1 h (Table 2). In Finland, Sweden, Norway and Estonia however, there is a larger increase in the median of the 20 summer maxima, which corresponds to the smaller CFs for the longer return period.

As the same behavior is seen in the underlying data (Table 3), the decline of CFs with longer return periods seems not to be a feature of the extrapolation in the GEV estimation. To further investigate the somewhat unexpected decline in CFs for the shortest durations, we have separated the AromeG data into its convective, stratiform and orographic-stratiform parts using the algorithm developed by Poujol et al. (2020) for convection permitting models. The separation (Table A2 and A3) shows that the changes in the stratiform part of the summer maxima is generally higher than in the convective part, and contrary to convection, also larger for the highest values than for the median. However, stratiform precipitation contributes only about 10–20% to the median and 5–10% to the highest summer maxima (not shown). As a result, the overall changes are dominated by changes in the convective contributions, especially for the highest, least frequent values.

Fig. 10 reveals a strong dependence between the 2-year return levels of 1-h precipitation estimated for the reference period 1986–2005 and the CFs for the same return period and duration, in both AromeE and AromeG simulations. CFs decrease with increasing return levels, and in areas that already experience high return levels CFs are constrained below ~1.5. A similar relationship is found for other durations and return periods (results not shown). A consequence of these changes might be more uniform 2-year return levels within the region. AromeG gives a larger spatial spread, with both higher values of the 2-year return levels, and higher CFs. This implies that AromeG not only projects a larger precipitation increase, probably due to higher climate sensitivity, but also simulates slightly larger heavy precipitation amounts in the current climate as seen in the maps in Fig. 3, at least for the 1 h duration.

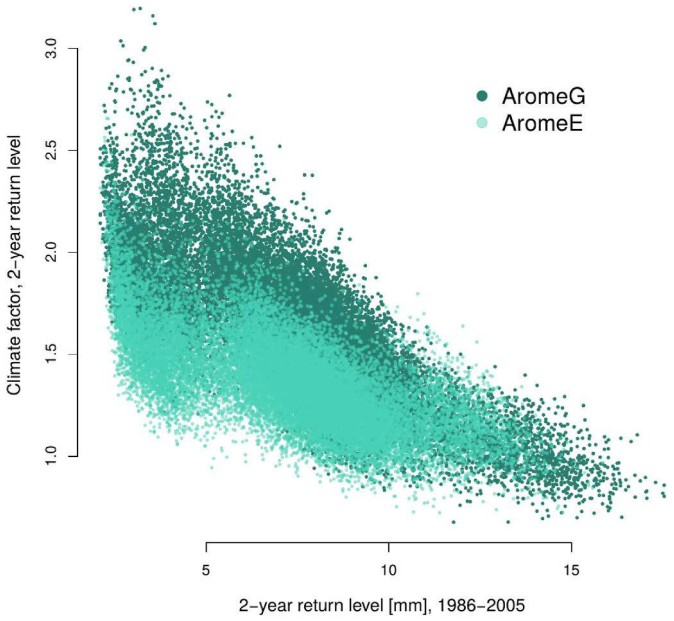

Fig. 10. Comparison between the summer 2-year return level for the reference period 1986–2005 and 1 h duration, as estimated from AromeG (dark green) and AromeE (light green) simulations, and the CFs for the same return period, duration and models. (For interpretation of the references to color in this figure legend, the reader is referred to the Web version of this article.)

Fig. 11 compares scaled CFs (see Equation (2)) based on AromeE, AromeG and WRF over Southern Norway. The similarity between CFs from AromeG and AromeE when scaled by North Europe ΔT reveals the high climate sensitivity of GFDL in this area. CFs scaled by the global ΔT are, however, much higher for AromeG. WRF estimates are lower for all durations when scaled by global ΔT, which could be related to the relatively strong decrease in summer precipitation projected by the driving GCM (CESM1-CAM4) compared to other CMIP5 models (Hodnebrog et al., 2019). CFs scaled by North Europe ΔT for the shortest durations are similar or higher compared to AromeE and AromeG.

In Fennoscandia, AROME gives lower CFs for 15 min compared to 1 h, while the opposite is true over the Baltic countries (Table 2) This is also evident from the scaled CFs in Fig. 11. WRF simulates a relatively linear increase in CFs with shorter durations, similar to the EC-ensemble. The difference between WRF and NorCP simulations in regards to duration dependence might lie in the use of shallow convection parameterization schemes. In Ban et al. (2021), CPM simulations that only differ in the choice of shallow convection parameterization scheme show very different magnitudes of heavy daily and hourly summer precipitation. The WRF simulations used here do not apply a shallow

Table 3
Median/maximum of the summer maxima of hourly precipitation from AromeG in the historical and future period and the resulting factor. The values have been calculated at each grid-point and averaged over the whole domain and for each country. *Italic: factor for the maximum < factor for the median.*

JJA max [mm/h]	Finland	Sweden	Norway	Denmark	Estonia	Latvia	Lithuania
1986–2005	9.5/22.6	9.8/21.9	8.7/19.7	11.4/26.3	12.1/30.0	14.3/31.8	15.7/34.9
2081–2 100	16.2/36.1	16.1/35.1	14.6/31.9	13.4/32.5	17.2/41.6	16.1/41.6	16.7/41.2
Factor	*1.7/1.6*	*1.6/1.6*	*1.7/1.6*	1.2/1.2	*1.4/1.4*	1.1/1.3	1.1/1.2

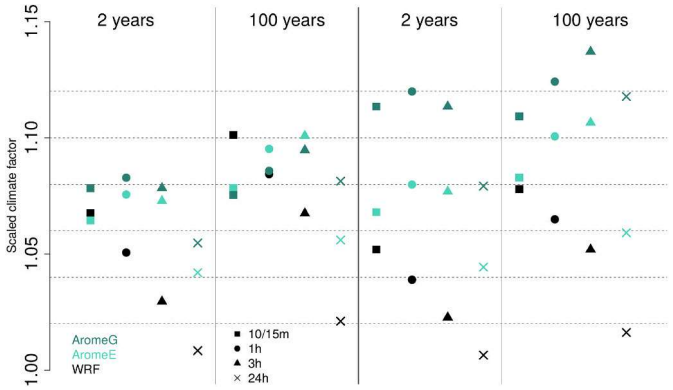

Fig. 11. Summer CFs for the 2-year and 100-year return levels scaled by the North Europe (left) and the global (right) 2 m-temperature increase from the driving GCM. CFs represent the limited domain over Southern Norway (Fig. 2) and the three convective permitting simulations; AromeG (dark green), AromeE (light green) and WRF (black). (For interpretation of the references to color in this figure legend, the reader is referred to the Web version of this article.)

parameterization scheme, while HCLIM38-AROME uses a shallow convection parameterization based on the eddy diffusivity mass-flux framework (EDMFm; de Rooy and Siebesma, 2008; Bengtsson et al., 2017).

Our results imply that changes with duration are mainly due to the CP model, while the overall magnitude of the climate factors is heavily influenced by the driving GCM.

This is supported by the results in Christensen and Kjellström (2020), Sørland et al. (2020) and Sørland et al. (2021) who found that the choice of GCM has the largest influence on the climate change signal. However, over complex terrain the choice of RCM starts to play a larger role as physical processes that e.g. influence the precipitation signal, are being (partly) resolved.

An increase in CFs with longer return periods is quite obvious in WRF simulations, with the exception of similar values for the 20 and 100-year return period and 24 h duration. AromeE simulates continuously increasing CFs with longer return periods, while AromeG simulates a slight decrease with longer return periods for the shortest duration. Apart from this the variability between durations is very similar between AromeE and AromeG.

4. Conclusions

As given in the Introduction, recommended climate change allowances for heavy precipitation in the Nordic countries vary between 1.20 and 1.50, somewhat depending on duration and return period. Results in the current study clearly suggest higher CFs with longer return period, with only few exceptions. The feature of lower CFs with longer return period is most evident in the AromeG simulation which also shows the most pronounced climate change signal. We suggest that this might be a result of projected changes being dominated by changes in the convective contributions, especially for the highest, least frequent values. We encourage a more detailed analysis of the convective and stratiform contributions in the RCM and CP simulations which could shed light on the underlying processes and reduce the uncertainty in the results. Particularly, some of the unexpected features in AromeG, like the strong latitudinal dependency of the CFs and the decline with longer return periods, should be further investigated. Also the role that moisture availability is playing in limiting summer maximum precipitation in the southern parts of the domain, as indicated in Ye et al. (2014) and Lind et al. (2022), should be subject for future research.

As to the dependence on duration, we found distinctly higher CFs going from daily to sub-daily durations, however, the different simulations give conflicting results for very short-duration rainfall (<3 h). NorCP simulations give increasing CFs between 24 h and sub-daily durations, but an overall decrease between 1 h and 15 min. Country-specific numbers show that this rather surprising feature is seen in the whole of Fennoscandia, representing the largest area, while in the three Baltic countries the CFs increase between 1 h and 15 min.

The heavy computational requirements of convection permitting simulations, resulting in small ensembles over a limited area and time period, is the case also for the NorCP simulations. The huge difference in the climate sensitivity of driving GCMs dominates the magnitude of estimated return levels. An ensemble of two model simulations, or three in the case of Southern Norway, will not encapture true model uncertainty. Nor will uncertainty in future emissions be represented by only one emission scenario. However, we argue that a holistic assessment of a combined dataset, with their different strengths and weaknesses, is a valuable exercise to reach robust climate change allowances.

CFs based on AromeE are similar to the median of the EURO-CORDEX ensemble, while CFs based on AromeG are much higher in some areas. An exception is Denmark, where AromeE is on the low side compared to the EC-ensemble, while AromeG gives CFs of around 1.20–1.30, similar to the current recommended climate change allowances. CFs for 1 h in Finland, Sweden and Norway given by AromeE and the EC-ensemble, lie around 1.30 for short return periods and around 1.40 for long return periods. In comparison, current climate change allowances in Finland (1.20) and Sweden (at least 1.20) appear on the low side, but one important difference is the consideration of lower emission scenarios in these countries' CF estimates (RCP4.5 for Sweden and A2 for Finland). The Norwegian climate change allowances are, on the other hand, based on the same emission scenario used here (RCP8.5), as the Norwegian government recommends using the high emission scenario (based on the precautionary principle) when assessing the effect of climate change. According to AromeG, particularly Latvia and Lithuania lie in areas of lowsmall CFs, suggesting limited changes in design precipitation.

Now, let's say we pursue one recommended number (climate change allowance) based on the following.

1. Two sets of simulations (convection permitting and non-convection permitting)
2. The two NorCP ensemble members; AromeE and AromeG, provide very different results
3. AromeE results are similar to the median of the non-convection permitting ensemble (EC-ensemble).

If we, in addition, take into account the enormous costs associated with adaptation measures that minimize future risk, i.e.considering the high end of estimated changes, and assume that the EURO-CORDEX ensemble properly simulates non-convective precipitation which dominates heavy precipitation over longer durations (>3 h), the CFs given by AromeE seem adequate. Furthermore, given the reduced damage risk already lying in the choice of a high emission scenario (RCP8.5), it seems reasonable not to determine climate change allowances based on a model with a significantly larger climate change signal (GFDL) compared to other models.

What happens at the very short durations is still not well understood and should be subject to further research. At what rate the most harmful downbursts, with very intense rainfall over a short amount of time, will intensify in the future, compared to the less intense events, is not clear. However, despite the limitations and, to a certain degree, conflicting results, we recommend that each country in the study region oversee their CF estimates and recommended climate change allowances, if any, in the light of new results from the current study.

Author statement

Erika Médus: Conceptualization, methodology, software, writing, reviewing and editing.

Anita Verpe Dyrrdal: Analysis, methodology, plotting, writing, original draft preparation.

Andreas Dobler: Analysis, methodology, plotting, writing, reviewing and editing.

Øivind Hodnebrog: Preparing and providing data, methodology, writing, reviewing and editing.

Karsten Arnbjerg-Nielsen: Writing, reviewing and editing.

Jonas Olsson: Writing, reviewing and editing.

Emma Dybro Thomassen: Writing, reviewing and editing.

Petter Lind: Writing, reviewing and editing.

Dace Gaile: Writing, reviewing and editing.

Piia Post: Writing, reviewing and editing.

Declaration of competing interest

The authors declare that they have no known competing financial interests or personal relationships that could have appeared to influence the work reported in this paper.

Data availability

Data will be made available on request.

Acknowledgement

We acknowledge the World Climate Research Programme's Working Group on Regional Climate, and the Working Group on Coupled Modeling, former coordinating body of CORDEX and responsible panel for CMIP5. We also thank the climate modeling groups (listed in Table A1 of this paper) for producing and making available their model output.

We would like to thank Ole Christensen and Peter Berg for providing the EURO-CORDEX data analyzed here, and specifically Dr. Heimo Truhetz from the University of Graz, Austria, for providing the MPI-CCLM data and Christian Steger from DWD for providing the MIROC-CCLM and CanESM-CCLM data.

This work uses data from the NorCP project, which is a Nordic collaboration involving climate modeling groups from the Danish Meteorological Institute (DMI), Finnish Meteorological Institute (FMI), Norwegian Meteorological Institute (MET Norway) and the Swedish Meteorological and Hydrological Institute (SMHI).

We acknowledge the Earth System Grid Federation infrastructure, an international effort led by the U.S. Department of Energy's Program for Climate Model Diagnosis and Intercomparison, the European Network for Earth System Modeling and other partners in the Global Organization for Earth System Science Portals (GO-ESSP).

The work of EM was funded by the Maj and Tor Nessling foundation.

JO wants to acknowledge the EDUCAS project (Swedish Research Council Formas, Grant no. 2019–00829).

The work of AVD and AD was partly funded by the Norwegian Centre for Climate Services, which again is partly funded by the Norwegian Ministry of Climate and Environment and the Norwegian Environment Agency. AVD would also like to acknowledge funding from the Research Council of Norway (Climdesign project; 302457).

ØH would like to acknowledge funding from the Research Council of Norway (275589).

Appendix A

Table A1
EURO-CORDEX models and modeling groups providing 1-h precipitation data.

GCM	RCM							
	RCA	CCLM	RACMO	HIRHAM	REMO	COSMO	ALADIN	RegCM
MIROC-**MIROC5**		r1/v1[1]						
CCCma-**CanESM2**		r1/v1[2]						
CNRM-CERFACS-**CNRM-CM5**				r1/v2[3]			r1/v2[4]	
ICHEC-**EC-EARTH**	r1/v1[5]		r1/v1[6]	r3/v1[7]				
MOHC-**HadGEM2-ES**	r1/v1[8]*		r1/v2[9]*				r1/v1[10]*	
IPSL-**IPSL-CM5A-MR**	r1/v1[11]							
MPI-***M*-MPI-ESM-LR**	r1/v1a[12]	r1/v1[13]		r1/v1[14]	r1/v1[15] r3/v1[16]	r1/v1[17]		r1/v1[18]
NCC-**NorESM1-M**	r1/v1[19]			r1/v3[20]		r1/v1[21]		

[1,2] CCLM4-8-17: CLM-Community/Deutscher Wetterdienst (DWD).
[3] HIRHAM5: Danish Meteorological Institute (DMI).
[4] ALADIN63: Centre National de Recherches Meteorologiques (CNRM).
[5+8+11+19] RCA4: Swedish Meteorological and Hydrological Institute (SMHI).
[6] RACMO22E: Koninklijk Nederlands Meteorologisch Instituut (KNMI).
[7+14] HIRHAM5: DMI.
[9] RACMO22E: KNMI.
[10] ALADIN63: CNRM.
[12] RCA4: SMHI.
[13] CCLM4-8-17: CLM-Community/Wegener Centre for Climate and Global Change (WEGC).
[15] REMO 2009: Climate Service Centre Germany (GERICS).
[16] REMO 2015: GERICS.
[17+21] COSMO-crCLIM-v1-1: CLM-Community/Eidgenössische Technische Hochschule (ETH) Zurich.
[18] RegCM4-6: International Centre for Theoretical Physics (ICTP).
[20] HIRHAM5: DMI.
*Note that all HadGEM-driven RCMs include only 2081–2099.

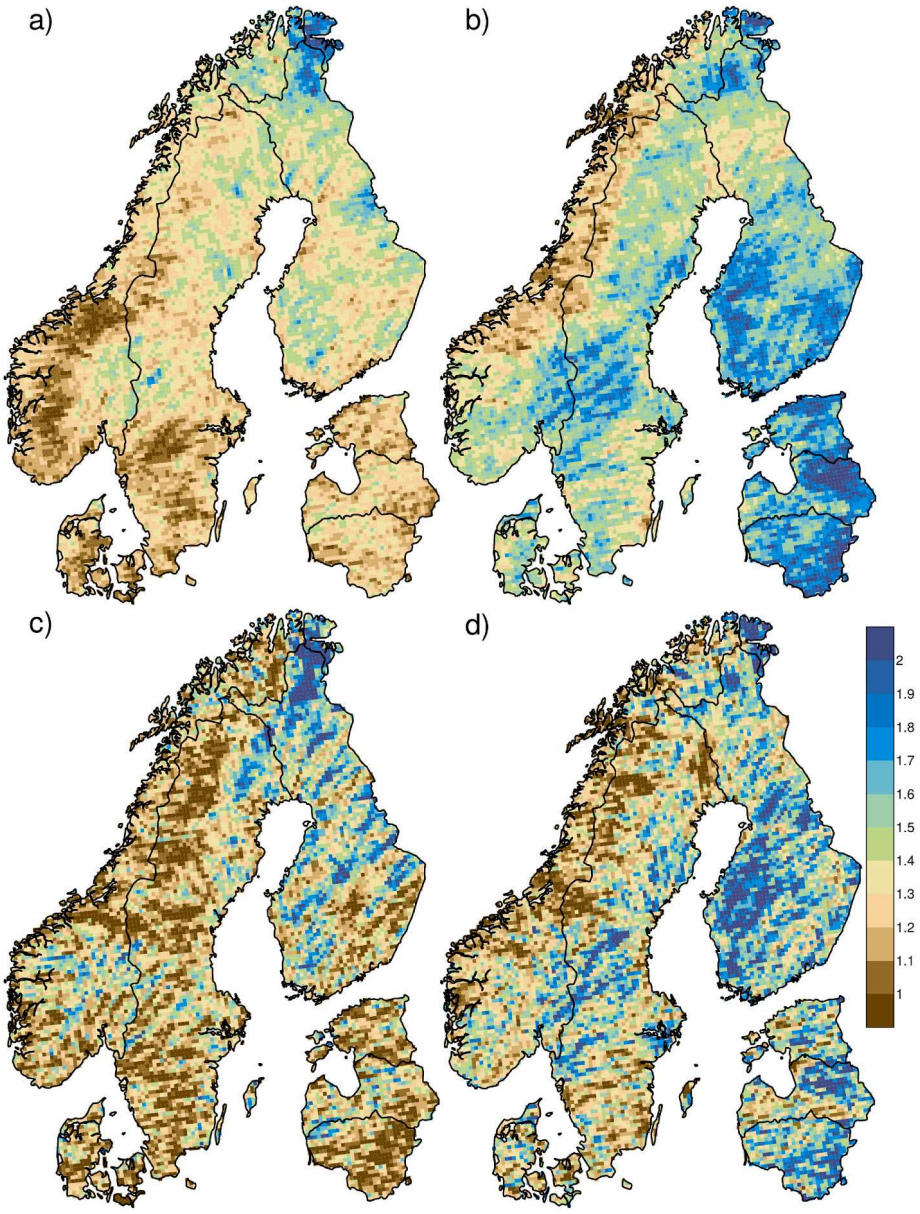

Fig. A1. Climate factors for 2-year (upper) and 100-year (lower) return levels for 1 h winter (DJF) precipitation, from AromeE (left) and AromeG (right).

Table A2
Median/maximum of the **convective** part of the summer maxima hourly precipitation in the historical and future AromeG simulation and the resulting CFs. The values have been calculated at each grid-point and averaged over the whole domain and for each country. *Italic: CFs for the maximum < CFs for the median.*

JJA-max [mm/h]	All	Finland	Sweden	Norway	Denmark	Estonia	Latvia	Lithuania
1986–2005	9.74/21.73	9.58/22.80	9.90/22.06	9.18/20.15	11.43/26.43	12.10/30.07	14.36/31.88	15.68/34.96
2081–2 100	13.31/31.45	16.30/36.17	16.18/35.23	14.80/31.99	13.40/32.51	17.19/41.66	16.10/41.50	16.73/41.18
CF	1.37/1.45	*1.70/1.59*	*1.63/1.60*	*1.61/1.59*	1.17/1.23	*1.42/1.39*	1.12/1.30	1.07/1.18

Table A3
Median/maximum of the **stratiform** part of the summer maxima hourly precipitation in the historical and future AromeG simulation and the resulting CFs. The values have been calculated at each grid-point and averaged over the whole domain and for each country. *Italic: CFs for the maximum < CFs for the median.*

JJA-max [mm/h]	All	Finland	Sweden	Norway	Denmark	Estonia	Latvia	Lithuania
1986–2005	6.05/13.56	9.14/20.67	9.67/21.14	7.97/17.84	11.15/24.46	11.73/27.07	14.04/30.99	15.36/33.87
2081–2 100	10.28/26.01	15.85/35.33	15.76/34.16	13.96/31.77	12.95/31.54	16.91/40.07	16.06/43.26	16.40/40.56
CF	1.70/1.92	*1.73/1.71*	*1.63/1.62*	1.75/1.78	1.16/1.29	1.44/1.48	1.14/1.40	1.07/1.20

References

Arnbjerg-Nielsen, K., 2012. Quantification of climate change effects on extreme precipitation used for high resolution hydrologic design. Urban Water J. 9 (2), 57–65. https://doi.org/10.1080/1573062X.2011.630091.

Arnbjerg-Nielsen, K., Leonardsen, L., Madsen, H., 2015. Evaluating adaptation options for urban flooding based on new high-end emission scenario regional climate model simulations. Clim. Res. 64, 73–84. https://doi.org/10.3354/cr01299.

Ban, N., Caillaud, C., Coppola, E., Pichelli, E., Sobolowski, S., Adinolfi, M., Ahrens, B., Alias, A., Anders, I., Bastin, S., Belusic, D., Berthou, S., Brisson, E., Cardoso, R.M., Chan, S.C., Christensen, O.B., Fernandez, J., Fita, L., Frisius, T., Gasparac, G., Giorgi, F., Goergen, K., Haugen, J.E., Hodnebrog, O., Kartsios, S., Katragkou, E., Kendon, E.J., Keuler, K., Lavin-Gullon, A., Lenderink, G., Leutwyler, D., Lorenz, T., Maraun, D., Mercogliano, P., Milovac, J., Panitz, H.J., Raffa, M., Remedio, A.R., Schar, C., Soares, P.M.M., Srnec, L., Steensen, B.M., Stocchi, P., Tolle, M.H., Truhetz, H., Vergara-Temprado, J., de Vries, H., Warrach-Sagi, K., Wulfmeyer, V., Zander, M.J., 2021. The first multi-model ensemble of regional climate simulations at kilometer-scale resolution, part I: evaluation of precipitation. Clim. Dynam. 28 https://doi.org/10.1007/s00382-021-05708-w.

Belušić, D., de Vries, H., Dobler, A., Landgren, O., Lind, P., Lindstedt, D., Pedersen, R.A., Sánchez-Perrino, J.C., et al., 2020. HCLIM38: a flexible regional climate model applicable for different climate zones from coarse to convection-permitting scales. Geosci. Model Dev. (GMD) 13, 1311–1333. https://doi.org/10.5194/gmd-13-1311-2020.

Benestad, R.E., Lussana, C., Lutz, J., Dobler, A., Landgren, O., Haugen, J.E., et al., 2022. Global hydro-climatological indicators and changes in the global hydrological cycle and rainfall patterns. PLOS Clim 1 (5), e0000029. https://doi.org/10.1371/journal.pclm.0000029.

Benestad, R.E., Parding, K.M., Erlandsen, H.B., Mezghani, A., 2019. A simple equation to study changes in rainfall statistics. Environ. Res. Lett. 14 (8) https://doi.org/10.1088/1748-9326/ab2bb2.

Bengtsson, L., Andrae, U., Aspelien, T., Batrak, Y., Calvo, J., de Rooy, W., Gleeson, E., Hansen-Sass, B., Homleid, M., Hortal, M., Ivarsson, K., Lenderink, G., Niemelä, S., Nielsen, K.P., Onvlee, J., Rontu, L., Samuelsson, P., Muñoz, D.S., Subias, A., Tijm, S., Toll, V., Yang, X., Køltzow, M.Ø., 2017. The HARMONIE–AROME model configuration in the ALADIN–HIRLAM NWP system. Mon. Weather Rev. 145 (5), 1919–1935. Retrieved Jul 7, 2022, from. https://journals.ametsoc.org/view/journals/mwre/145/5/mwr-d-16-0417.1.xml.

Christensen, O.B., Kjellström, E., 2020. Partitioning uncertainty components of mean climate and climate change in a large ensemble of European regional climate model projections. Clim Dyn 54, 4293–4308. https://doi.org/10.1007/s00382-020-05229-y.

Christensen, O.B., Kjellström, E., Dieterich, C., Gröger, M., Meier, H.E.M., 2022. Atmospheric regional climate projections for the Baltic Sea region until 2100. Earth Syst Dyn 13, 133–157. https://doi.org/10.5194/ESD-13-133-2022.

Coles, S.G., 2001. An Introduction to Statistical Modeling of Extreme values. Springer Series in Statistics.

DMI, 2018. Vejledning I Anvendelse Af Udledningsscenarier (in Danish). Danish Meteorological Institute.

Donner, L.J., Wyman, B.L., Hemler, R.S., others, 2011. The dynamical core physical parameterizations, and basic simulation characteristics of the atmospheric component AM3 of the GFDL global coupled model CM3. J. Clim. 24, 3484–3519. https://doi.org/10.1175/2011jcli3955.1.

Dyrrdal, A.V., Olsson, J., Médus, E., Arnbjerg-Nielsen, K., Post, P., Aņiskeviča, S., Thorndahl, S., Førland, E., Wern, L., Mačiulytė, V., Mäkelä, A., 2021. Observed changes in heavy daily precipitation over the Nordic-Baltic region. J. Hydrol.: Reg. Stud. 38, 100965 https://doi.org/10.1016/j.ejrh.2021.100965. ISSN 2214-5818.

Fowler, H.J., Wasko, C., Prein, A.F., 2021. Intensification of short-duration rainfall extremes and implications for flood risk: current state of the art and future directions. Philos. Trans. A. Math. Phys.. Eng. Sci. 379 (2195), 20190541. https://doi.org/10.1098/rsta.2019.0541. Epub 2021 Mar 1. PMID: 33641465; PMCID: PMC8366905.

Gent, P.R., Danabasoglu, G., Donner, L.J., Holland, M.M., Hunke, E.C., Jayne, S.R., Lawrence, D.M., Neale, R.B., Rasch, P.J., Vertenstein, M., Worley, P.H., Yang, Z.L., Zhang, M.H., 2011. The community climate system model version 4. J. Clim. 24 (19), 4973–4991. https://doi.org/10.1175/2011jcli4083.1.

Griffies, S.M., Winton, M., Donner, L.J., others, 2011. The GFDL CM3 coupled climate model: characteristics of the ocean and Sea ice simulations. J. Clim. 24, 3520–3544. https://doi.org/10.1175/2011jcli3964.1.

Hazeleger, W., Wang, X., Severijns, C., others, 2011. EC-Earth V2.2: description and validation of a new seamless earth system prediction model. Clim. Dynam. 39, 2611–2629. https://doi.org/10.1007/s00382-011-1228-5.

Hodnebrog, Ø., Marelle, L., Alterskjær, K., Wood, R.R., Ludwig, R., Fischer, E.M., Richardson, T.B., Forster, P.M., Sillmann, J., Myhre, G., 2019. Intensification of summer precipitation with shorter time-scales in Europe. Environ. Res. Lett. 14, 124050. https://iopscience.iop.org/article/10.1088/1748-9326/ab549c.

IPCC, 2021. Summary for policymakers. In: Zhai, P., Pirani, A., Connors, S.L., Péan, C., Berger, S., Caud, N., Chen, Y., Goldfarb, L., Gomis, M.I., Huang, M., Leitzell, K., Lonnoy, E., Matthews, J.B.R., Maycock, T.K., Waterfield, T., Yelekçi, O., Yu, R., Zhou, B. (Eds.), Climate Change 2021: the Physical Science Basis. Contribution of Working Group I to the Sixth Assessment Report of the Intergovernmental Panel on Climate Change [Masson-Delmotte, V. Cambridge University Press, Cambridge, United Kingdom and New York, NY, USA, pp. 3–32. https://doi.org/10.1017/9781009157896.001.

Jacob, D., Petersen, J., Eggert, B., Alias, A., Christensen, O.B., Bouwer, L.M., Braun, A., Colette, A., Déqué, M., Georgievski, G., Georgopoulou, E., Gobiet, A., Menut, L., Nikulin, G., Haensler, A., Hempelmann, N., Jones, C., Keuler, K., Kovats, S., Kröner, N., Kotlarski, S., Kriegsmann, A., Martin, E., van Meijgaard, E., Moseley, C., Pfeifer, S., Preuschmann, S., Radermacher, C., Radtke, K., Rechid, D., Rounsevell, M., Samuelsson, P., Somot, S., Soussana, J.-F., Teichmann, C., Valentini, R., Vautard, R., Weber, B., Yiou, P., 2014. EURO-CORDEX: new high-resolution climate change projections for European impact research. Reg. Environ. Change 14 (2), 563–578.

Kendon, E.J., Ban, N., Roberts, N.M., Fowler, H.J., Roberts, M.J., Chan, S.C., Evans, J.P., Fosser, G., Wilkinson, J.M., 2017. Do convection-permitting regional climate models improve projections of future precipitation change? Bull. Am. Meteorol. Soc. 98 (1), 79–93. https://doi.org/10.1175/bams-d-15-0004.1.

Kuntaliitto (Association of Finnish Local and Regional Authorities), 2012. Hulevesiopas (Stormwater management guide. In: Finnish), p. 262. https://www.kuntaliitto.fi/asiantuntijapalvelut/yhdyskunnat-ja-ymparisto/tekniikka/hulevesien-hallinta/hulevesiopas.

Lind, P., Belušić, D., Christensen, O.B., Dobler, A., Kjellström, E., Landgren, O., Lindstedt, D., Matte, D., Pedersen, R.A., Toivonen, E., Wang, F., 2020. Benefits and added value of convection-permitting climate modeling over Fenno-Scandinavia. Clim. Dynam. 55, 1893–1912. https://doi.org/10.1007/s00382-020-05359-3.

Lind, P., Belušić, D., Médus, E., Dobler, A., Pedersen, R.A., Wang, F., Matte, D., Kjellström, E., Landgren, O., Lindstedt, D., Christensen, O.B., Christensen, J.H., 2022. Climate change information over Fenno-Scandinavia produced with a convection-permitting climate model. Clim. Dynam. https://doi.org/10.1007/s00382-022-06589-3.

Lind, P., Lindstedt, D., Kjellström, E., Jones, C., 2016. Spatial and temporal characteristics of summer precipitation over central Europe in a suite of high-resolution climate models. J. Climate 29, 3501–3518. https://doi.org/10.1175/JCLI-D-15-0463.1.

Lucas-Picher, P., Argüeso, D., Brisson, E., Tramblay, Y., Berg, P., Lemonsu, A., Kotlarski, S., Caillaud, C., 2021. Convection-permitting modeling with regional climate models: latest developments and next steps. Wiley Interdisciplinary Reviews: Clim. Change 12 (6), e731. https://doi.org/10.1002/wcc.731.

Madsen, H.M., Andersen, M.M., Rygaard, M., Mikkelsen, P.S., 2018. Definitions of event magnitudes, spatial scales, and goals for climate change adaptation and their importance for innovation and implementation. Water Res. 144, 192–203. https://doi.org/10.1016/j.watres.2018.07.026.

Marelle, L., Myhre, G., Hodnebrog, O., Sillmann, J., Samset, B.H., 2018. The changing seasonality of extreme daily precipitation. Geophys. Res. Lett. 45 (20), 11352–11360. https://doi.org/10.1029/2018gl079567.

Martins, E.S., Stedinger, J.R., 2000. Generalized maximum-likelihood generalized extreme-value quantile estimators for hydrologic data. Water Resour. Res. 36, 737–744. https://doi.org/10.1029/1999WR900330.

Matte, D., Christensen, J.H., Ozturk, T., 2022. Spatial extent of precipitation events: when big is getting bigger. Clim. Dynam. 58, 1861–1875. https://doi.org/10.1007/s00382-021-05998-0.

Médus, E., Thomassen, E.D., Belušić, D., Lind, P., Berg, P., Christensen, J.H., Christensen, O.B., Dobler, A., Kjellström, E., Olsson, J., Yang, W., 2022. Characteristics of precipitation extremes over the Nordic region: added value of convection-permitting modeling. Nat. Hazards Earth Syst. Sci. 22, 693–711. https://doi.org/10.5194/nhess-22-693-2022.

Meehl, G.A., Washington, W.M., Arblaster, J.M., Hu, A., Teng, H., Tebaldi, C., Sanderson, B.N., Lamarque, J., Conley, A., Strand, W.G., White III., J.B., 2012. Climate system response to external forcings and climate change projections in CCSM4. J. Clim. 25 (11), 3661–3683. https://doi.org/10.1175/JCLI-D-11-00240.1.

Myhre, G., Alterskjær, K., Stjern, C.W., Hodnebrog, Ø., Marelle, L., Samset, B.H., Sillmann, J., Schaller, N., Fischer, E., Schulz, M., Stohl, A., 2019. Frequency of extreme precipitation increases extensively with event rareness under global warming. Sci. Rep. 9 (1), 16063 https://doi.org/10.1038/s41598-019-52277-4.

NVE, 2022. NVE Veileder nr. 4/2022 Rettleiar for handtering av overvatn i arealplanar Korleis ta omsyn til vassmengder? (in Norwegian), Norwegian Water Resources and Energy directorate. In: Bakken Pedersen, T., Bratlie, R. (Eds.). https://publikasjoner.nve.no/veileder/2022/veileder2022_04.pdf.

Olsson, J., Berg, P., Eronn, A., Simonsson, L., Södling, J., Wern, L., Yang, W., 2017. Extremregn i nuvarande och framtida klimat (Extreme rainfall in present and future climate). Klimatologi 47 (SMHI, Sweden).

Olsson, J., Södling, J., Berg, P., Wern, L., Eronn, A., 2019. Short-duration rainfall extremes in Sweden: a regional analysis. Nord. Hydrol 50 (3), 945–960. https://doi.org/10.2166/nh.2019.073, 2019.

Olsson, J., Du, Y., An, D., Uvo, C.B., Sörensen, J., Toivonen, E., Belušić, D., Dobler, A., 2021. An analysis of (Sub-)Hourly rainfall in convection-permitting climate simulations over southern Sweden from a user's perspective. Front. Earth Sci. 9 https://doi.org/10.3389/feart.2021.681312.

Olsson, J., Dyrrdal, A.V., Médus, E., Södling, J., Aniskeviča, S., Arnbjerg-Nielsen, K., Førland, E., Mačiulytė, V., Mäkelä, A., Post, P., Thorndahl, S.L., Wern, L., 2022. Sub-daily rainfall extremes in the Nordic-Baltic region. Nord. Hydrol 53 (6), 807–824. https://doi.org/10.2166/nh.2022.119, 2022.

Parding, K.M., Dobler, A., McSweeney, C.F., others, 2020. GCMeval – an interactive tool for evaluation and selection of climate model ensembles. Climate Services 18, 100167. https://doi.org/10.1016/j.cliser.2020.100167.

Poujol, B., Sobolowski, S., Mooney, P., Berthou, S., 2020. A physically based precipitation separation algorithm for convection-permitting models over complex topography. Q. J. R. Meteorol. Soc. 146, 748–761. https://doi.org/10.1002/qj.3706.

Prein, A.F., Langhans, W., Fosser, G., Ferrone, A., Ban, N., Goergen, K., Keller, M., Toelle, M., Gutjahr, O., Feser, F., Brisson, E., Kollet, S., Schmidli, J., van Lipzig, N.P. M., Leung, R., 2015. A review on regional convection-permitting climate modeling: demonstrations, prospects, and challenges. Rev. Geophys. 53 (2), 323–361. https://doi.org/10.1002/2014rg000475.

Rooy, W.C., Siebesma, A.P., 2008. A simple parameterization for detrainment in shallow cumulus. Mon. Weather Rev. 136, 560–576. https://doi.org/10.1175/2007MWR2201.1.

Sillmann, J., Stjern, C.W., Myhre, G., Samset, B.H., Hodnebrog, O., Andrews, T., Boucher, O., Faluvegi, G., Forster, P., Kasoar, M.R., Kharin, V.V., Kirkevag, A., Lamarque, J.F., Olivie, D.J.L., Richardson, T.B., Shindell, D., Takemura, T., Voulgarakis, A., Zwiers, F.W., 2019. Extreme wet and dry conditions affected differently by greenhouse gases and aerosols. Npj Climate and Atmospheric Science 2 (7). https://doi.org/10.1038/s41612-019-0079-3.

Skamarock, W.C., Klemp, J.B., 2008. A time-split nonhydrostatic atmospheric model for weather research and forecasting applications. J. Comput. Phys. 227, 3465–3485.

Sørland, S.L., Brogli, R., Pothapakula, P.K., Russo, E., Walle, J.V.d., Ahrens, B., et al., 2021. COSMO-CLM regional climate simulations in the CORDEX framework: a review. Geosci. Model Dev 14, 5125–5154. https://doi.org/10.5194/gmd-14-5125-2021.

Sørland, S.L., Fischer, A.M., Kotlarski, S., Künsch, H.R., Liniger, M.A., Rajczak, J., et al., 2020. CH2018—national climate scenarios for Switzerland: how to construct consistent multi-model projections from ensembles of opportunity. Climate Ser. 20, 100196.

Sorteberg, A., Lawrence, D., Dyrrdal, A.V., Mayer, S., 2018. Engeland Climatic Changes in Short Duration Extreme Precipitation and Rapid Onset Flooding - Implications for Design Values. NCCS report no.1/2018. www.klimaservicesenter.no.

Spildevandskomiteen, 2014. Opdaterede Klimafaktorer Og Dimensionsgivende Regnintensiteter, Skrift Nr. 30, Spildevandskomiteen, Ingeniørforeningen I Danmark – IDA. https://ida.dk/media/2994/svk_skrift30_0.pdf.

Tamm, O., Saaremäe, E., Rahkema, K., Jaagus, J., Tamm, T., 2023. The intensification of short-duration rainfall extremes due to climate change – need for a frequent update of intensity–duration–frequency curves. Climate Services 30 (2023), 100349. https://doi.org/10.1016/j.cliser.2023.100349. ISSN 2405-8807.

van Oldenborgh, G.J., M, C., Arblaster, J., Christensen, J., Marotzke, J., Power, S., Rummukainen, M., Zhou, T., 2013. In: Stocker, T.F., Qin, D., Plattner, G.-K., Tignor, M., Allen, S.K., Boschung, J., Nauels, A., Xia, Y., Bex, V., Midgley, P.M. (Eds.), Climate Change 2013: the Physical Science Basis. Contribution of Working Group I to the Fifth Assessment Report of the Intergovernmental Panel on Climate Change, Book Section Annex I: Atlas of Global and Regional Climate Projections. Cambridge University Press, Cambridge, United Kingdom and New York, NY, USA, pp. 1311–1394. https://doi.org/10.1017/CBO9781107415324.029. www.climatechange2013.org.

Vatten, Svenskt, 2016. Avledning Av Dag-, Drän- Och Spillvatten (Diversion of Storm, Drain and Waste Water). Publication P110, Svenskt Vatten, Stockholm, Sweden.

Westra, S., Fowler, H.J., Evans, J.P., Alexander, L.V., Berg, P., Johnson, F., Kendon, E.J., Lenderink, G., Roberts, N.M., 2014. Future changes to the intensity and frequency of short-duration extreme rainfall. Rev. Geophys. 52, 522–555. https://doi.org/10.1002/2014RG000464.

Willems, P., Arnbjerg-Nielsen, K., Olsson, J., Nguyen, V.T.V., 2012. Climate change impact assessment on urban rainfall extremes and urban drainage: methods and shortcomings. Atmos. Res. 103, 106–118. https://doi.org/10.1016/j.atmosres.2011.04.003.

Ye, H., Fetzer, E.J., Wong, S., Behrangi, A., Olsen, E.T., Cohen, J., Lambrigtsen, B.H., Chen, L., 2014. Impact of increased water vapor on precipitation efficiency over northern Eurasia. Geophys. Res. Lett. 41 (8), 2941–2947. https://doi.org/10.1002/2014GL059830.